Macromolecules

Article

pubs.acs.org/Macromolecules

Nanoparticle Diffusion in Methycellulose Thermoreversible Association Polymer

Ah-Young Jee,[†] Jaime L. Curtis-Fisk,[⊥] and Steve Granick*[,†,‡,§,∥]

[†]Departments of Materials Science and Engineering, [‡]Chemical and Biomolecular Engineering, [§]Chemistry, and [∥]Physics, University of Illinois, Urbana, Illinois 61801, United States

[⊥]The Dow Chemical Company, Midland, Michigan 48674, United States

ABSTRACT: Solutions of aqueous methylcellulose, a hydrophobically modified polymer (molecular weight ≈270 kg/mol, methyl content ≈30%), are mixed with either dilute coumarin fluorescent dye or carboxylated latex (20 nm diameter), and the tracer diffusion is contrasted as a function of temperature and polymer concentration (from dilute to 36 times the overlap concentration) in deionized water. From two-photon fluorescence correlation spectroscopy (FCS), mean-square displacement is inferred. At room temperature, which is the fluid state, we observe Fickian diffusion provided that the tracer particle size is less than the polymer mesh size, whereas tighter meshes produce subdiffusion followed by Fickian diffusion at long times. At elevated temperature, which is the gel state, subdiffusion is observed over the entire experimental time window. To quantify subdiffusion, the data are described equally well as two discrete relaxations or a stretched exponential, and the former is analyzed in detail as it is considered to be more meaningful physically. These measurements allow us to discuss the structure and degree of inhomogeneity of methylcellulose in the gel state. This industrially relevant polymer produces simple, physically meaningful diffusion patterns that we find to be repeatable, obeying systematic patterns described quantitatively in this paper.

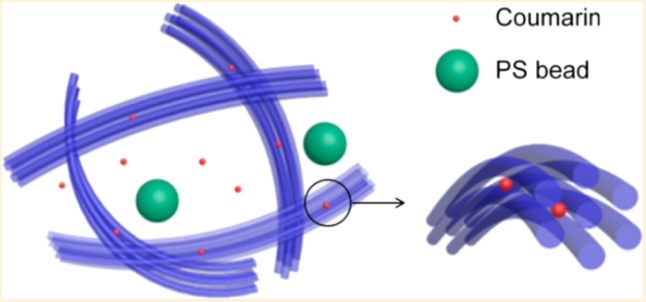

The extraordinary solubilization properties of aqueous association polymers enable interesting technologies in a diverse range of fields, among them the food and pharmaceutical industries. The interaction of polymer gels with other components in the solution has impact on properties such as solubilization and diffusion and therefore on functional performance of the system. Here we are interested from the polymer physics perspective in association polymers based on hydrophobic modification of the raw natural material, methylcellulose (MC).[1] This and another major class of association polymer, poly(ethylene oxide) (PEO)−poly(propylene oxide) (PPO) triblock copolymers (PEO−PPO−PEO),[2] share the feature of thermoreversibility between solution and gel state upon cooling and heating. Much progress has already come from studying how structural changes show up in rheological and thermal properties.[3−5] Here we are interested in a different question: what determines the mobility of solutes in association polymer?

It is known that the transport of nano- and micrometer-sized particles through random media when the particle size is much smaller than the correlation length (ξ) depends simply on the solvent viscosity as the medium then behaves as an isotropic fluid.[6,7] In such cases, the mean-square displacement (MSD) grows in proportion to time, $\langle r^2(t)\rangle \propto t^x$, such that $x = 1$ indicates Fickian diffusion behavior. But when tracer particles move in a crowded macromolecular environment or a concentrated polymer solution, they can be transiently caged,[8,9] resulting in a nonlinear relation between the MSD of the tracer and time, with $x < 1$. For gels, the mobility of tracer particles depends on the ratio of the size of the tracer particles to the mesh size of the network. In this manner, the gel structure can be probed at different scales by using tracer particles of various sizes. A detailed understanding of the diffusion of the tracer particles would allow one to determine the relationship between the macroscopic and microscopic viscosities of solutions and their gel structure.

Fluorescence correlation spectroscopy (FCS)[10,11] is well suited for such study owing to its high sensitivity and selectivity. It is conveniently applied to tracer particles in the range 1−150 nm, a range that is comparable to the mesh size of hydrogel. FCS measures the fluctuations in the fluorescence intensity that result from the diffusion of fluorophores in and out of the observed volume. Generally, the diffusion coefficient of the tracer in pure and diluted polymer solutions can be obtained simply by fitting the autocorrelation curve using a one-component model of free, Fickian diffusion.[12] However, sometimes the mobility of the tracer cannot be attributed in this way to a single Fickian process, perhaps owing to heterogeneous porous structure[13] or tracer interaction with the host.[14,15] We found that data in the gelled system, and in the fluid system when the polymer concentration was high,

Received: June 27, 2014
Revised: August 5, 2014

   dx.doi.org/10.1021/ma501331z | *Macromolecules* XXXX, XXX, XXX−XXX

demanded a more complex fit than just a single component. While the data could also be described empirically by the stretched exponential relationship, it was described equally well as the sum of two independent Fickian diffusion processes. The latter we consider to be more meaningful physically. Adopting this interpretation, our results show the appearance of two components when the tracer size exceeds the correlation length of the polymer solution. However, the finding of single-component diffusion in dilute solution was robust and was observed to persist for the carboxylated PS beads for periods of up to several days, confirming the absence of specific chemical attractions to methylcellulose.

RESULTS AND DISCUSSION

Methylcellulose (MC), trade name METHOCEL A4M, was provided by the Dow Chemical Company. The molecular weight, evaluated in the Dow research laboratories using triple detection size exclusion chromatography (Tri-SEC) and calibration using pullulan standards, was 270 kg/mol.[16] The MC solutions were prepared by fully dispersing the powder in 80 °C water with stirring for 1 h. The temperature was then decreased to 4 °C by placing the sample in an ice bath while continuing stirring, followed by overnight storage at 4 °C to complete hydration of the polymer. The overlap concentration (c^*) of MC, defined as the inverse of the intrinsic viscosity ($[\eta]$),[17] was 1.4 mg/mL. At each concentration (c), the corresponding correlation length of the solution (ξ) was evaluated by the standard relation[18] $\xi \approx R_g(c/c^*)^{-0.75}$ with R_g = 37.8 nm determined from an earlier study with similar polymer samples.[16]

We prepared polymer solutions in the range $0.5 \leq c/c^* \leq 36.5$. For investigation of tracer diffusion, we used coumarin fluorescent dye, hydrodynamic radius of approximately 0.5 nm, and also 20 nm diameter polystyrene (PS) beads (Invitrogen). The diffusion measurements were performed using a home-built FCS system[19] with two-photon excitation achieved using a femtosecond Ti:sapphire laser at wavelength 800 nm. The vertically polarized laser beam was split into two beams, one of which was introduced into an objective lens (LD-neofluar, 63×, numerical aperture = 0.67). Care was taken to focus the laser deep into the sample to avoid possible wall effects. To come up with each of the data points reported below, measurements were made at roughly 50 different spatial positions and averaged. The variation was typically less than 10%.

We began by studying solutions at room temperature, which is far below the gelation temperature of methylcellulose. The normalized fluorescence fluctuation autocorrelation function was calculated as $G(t) = (\langle \delta F(t)\delta F(t+\tau)\rangle)/\langle F(t)\rangle^2$, where $\delta F(t)$ is the difference between the fluorescence intensity at time t and its average value. Figure 1 shows this function for coumarin and PS beads in solutions of various polymer concentrations. The physical meaning of $G(t)$ is to quantify the time taken by a fluorophore to diffuse across the confocal volume. The diffusion coefficient (D_i) of each of the diffusion processes was evaluated as

$$G(t) = \frac{1}{N}\sum_{i=1}^{n} f_i \left[\left(1 + \frac{8D_i t}{w_{x,y}^2}\right)^{-1}\left(1 + \frac{8D_i t}{w_z^2}\right)^{-0.5}\right] \quad (1)$$

where $w_{x,y}$ and w_z are the calibrated dimensions of the observed volume perpendicular to and along the optical axis, respectively, and f is the relative fraction of each component. The values of

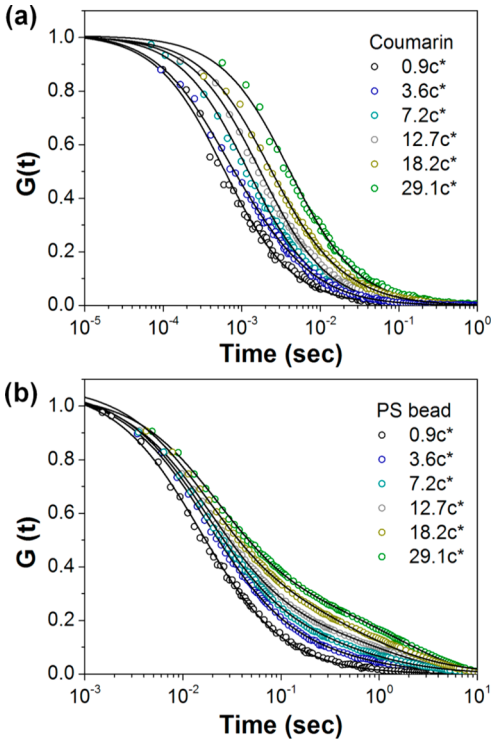

Figure 1. On linear−log scales, the normalized autocorrelation curve, $G(t)$, is plotted against time at room temperature for (a) coumarin and (b) carboxylated PS beads (20 nm) at various concentrations of aqueous methylcellulose, normalized to the overlap concentration c^* as indicated. The circles show the raw data. The solid lines show curves fitted using eq 1.

$w_{x,y}$ (300 nm) and w_z (8 μm) were calibrated from measuring the diffusion of the dye Rh6G and comparing it to the known values.[20]

When the particle size was less than ξ, the autocorrelation function $G(t)$ was described well by a single diffusion coefficient, as can be seen from the curves for coumarin (Figure 1a). In these instances the ξ ranged from 50 to 2.6 nm for methylcellulose solutions whose concentration was $0.5 \leq c/c^* \leq 36.5$. Equivalently, $G(t)$ can be expressed as the mean-square displacement (MSD) of position (r) as a function of time (t).[21] Plotting MSD against t on log−log scales, one finds the slope of $x = 1$.

For comparison, Figure 1b illustrates $G(t)$ of the larger carboxylated latex beads. As can be seen even qualitatively from the rightward shifts of the $G(t)$ curves, their diffusion slowed with increasing methylcellulose concentration. Single-component diffusion described this data up to $2.7c^*$, which is the condition under which the particle size was less than ξ. At higher methylcellulose concentrations the data implied two diffusion coefficients: one of them relatively fast (D_{fast}) and the other one slower (D_{slow}).

The implied mean-square displacement is plotted in Figure 2 against time on log−log scales. The single-component Fickian diffusion of coumarin is manifested as linear dependence on time, ($\langle \Delta r^2(t)\rangle \propto t$), as can be seen from Figure 2a. As for the latex particles, Figure 2b shows single-component diffusion in the low-concentration regime, $c/c^* < 2.7$, but two-component diffusion when the concentration was higher, the transition point coinciding with the point where PS particle size exceeded the correlation length of the methylcellulose solution. This was

dx.doi.org/10.1021/ma501331z | Macromolecules XXXX, XXX, XXX−XXX

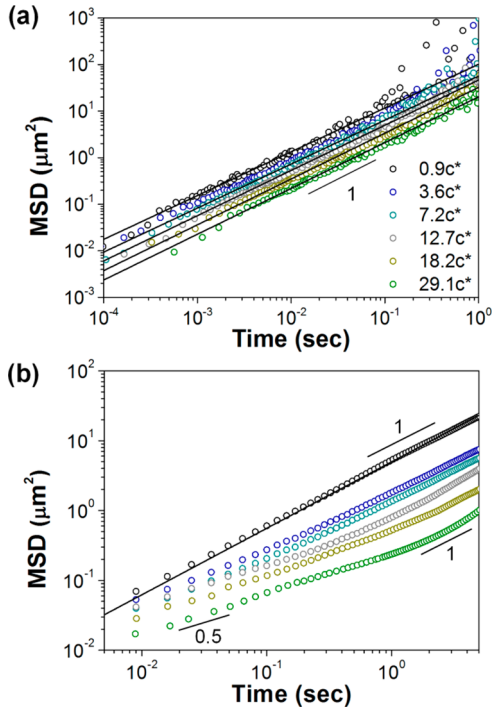

Figure 2. On log–log scales, the mean-square displacement (MSD) inferred from the autocorrelation curves in Figure 1 is plotted against time for (a) coumarin and (b) carboxylated PS beads (20 nm). Symbols are same as in Figure 1.

manifested in a regime of relatively short-time diffusion during which the PS particles displayed $\langle \Delta r^2(t) \rangle \sim t^x$ with $x \approx 0.9$–0.5, depending on the concentration of methylcellulose, presumably reflecting caging of some kind. This subdiffusive motion continued until fluctuations in the local mesh allowed the particles to move further.[22] At this point, the motion of the PS particles became Fickian with $x = 1.0$.

To understand further the decrease in the tracer diffusion coefficient (D) with increasing polymer concentration, we normalized the tracer diffusion coefficient to the diffusion coefficient corresponding to the pure solvent environment, D_0 (Figure 3). For coumarin, the diffusion coefficient remained constant in the very dilute regime up to c^*, and then it decreased strongly. The normalized values corresponding to

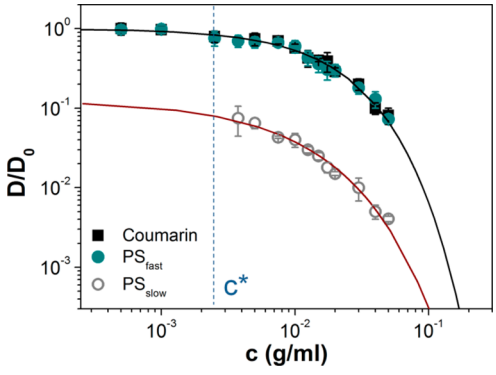

Figure 3. On log–log scales, the relative diffusivity D/D_0 is plotted against methylcellulose concentration for coumarin (black line), for the fast diffusion component of 20 nm carboxylated beads (black line), and for the slow diffusion component of 20 nm carboxylated beads (red line).

coumarin were described by a single master curve. To describe the dependence on polymer concentration,[23] the data could be parametrized using the stretched exponential function, $D/D_0 = \exp(-\alpha c^{\beta})$, with $\alpha = 40$ and $\beta = 0.9$. Remarkably, the D_{fast} of PS latex particles could be superimposed on the same master curve. This fully described the data for methylcellulose concentrations up to $2.7c^*$, for which only the D_{fast} existed, and for higher methylcellulose concentrations it described the data indicative of the diffusion of the PS particles after, having escaped caging, their diffusion was affected only by the viscosity of the polymer solution.[22] Parenthetically, we note that the diffusion of these particles in the subdiffusive regime was also described satisfactorily by a stretched exponential relation with $\alpha = 32$ and $\beta = 0.7$ although the range of the data is small. These values of the exponent β are similar to those reported from other studies in other polymer systems.[24−26] In this study, we pursued analysis in terms of two-component diffusion as, in our view, it offers more physical meaning for the system under study here.

Next, we studied the diffusion of tracers after heating to temperatures past the gel point. Two methylcellulose concentrations were studied, $1.8c^*$ and $7.2c^*$, at temperatures from 25 to 70 °C. As shown in Figure 4a, for coumarin dye the one-component diffusivity (low temperature) switched to two-component at 60 and 55 °C for the methylcellulose concentrations of $1.8c^*$ and $7.2c^*$, respectively, which are the gelation temperatures for those concentrations. PS beads showed the same trend at methylcellulose concentration $1.8c^*$ such that the methylcellulose correlation length (ξ) exceeded the bead size, but the fast-diffusion coefficient decreased significantly above gelation temperature (Figure 4b). On the other hand, at methylcellulose concentration of $7.2c^*$ such that the ξ was smaller than the bead size, two-component diffusion was observed starting already at low temperature; both components slowed down when the methylcellulose switched to the gel state. This difference of physical response, depending on size of the tracer, suggests the hypothesis that the size of the tracer can be used to probe the gel structure.

We turn to diffusion in the gel state of methylcellulose. The experiments were performed at 70 °C, which is the gelation temperature at c^*, the lowest concentration that we studied. It was not possible to study gelation at lower concentration, as dilute solutions do not gel upon heating.[27] The autocorrelation curves of coumarin for a wide range of polymer concentrations are shown in Figure 5a. The autocorrelation curves show slower diffusion than at lower temperature and now are composed of two components, as can be seen from the plot of residuals (inset). Figure 5b discriminates the two apparent diffusion coefficients: the D_{fast} value of coumarin decreases with increasing polymer concentration, while D_{slow} is independent of polymer concentration. In addition, the contribution of the slow component increases with polymer concentration, from ≈10% (2.5 mg/mL polymer) to ≈35% at the highest polymer concentrations. Note that these measurements were made deep within the gel phase. The FCS measurement captures signal only at the point of focus; the light path entering and leaving does not contribute to the signal. Therefore, the known syneresis of methylcellulose cannot explain the observation of two-component diffusion.

In this context, we note the recent report that in the process of methylcellulose gelation initially the chains aggregate into bundles (fibrils), and then these fibrils assemble into a network

dx.doi.org/10.1021/ma501331z | Macromolecules XXXX, XXX, XXX–XXX

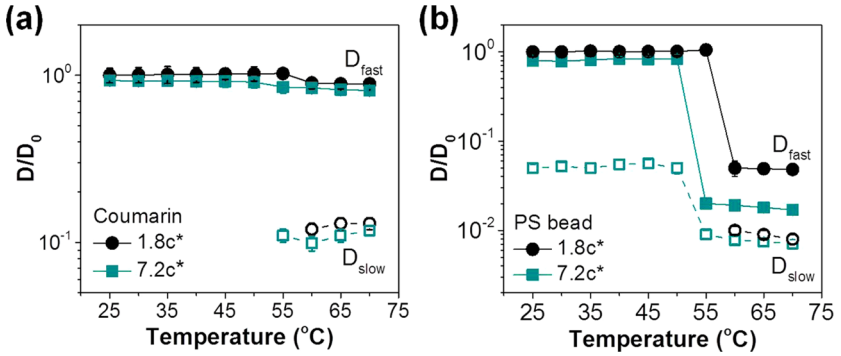

Figure 4. On log−linear scales, the relative diffusivity (D/D_0) of (a) coumarin and (b) carboxylated PS beads plotted against temperature at methylcellulose concentration 1.8c* (black circles) and 7.2c* (green squares). Filled and empty symbols show fast and slow diffusion coefficients from two-component fitting, respectively.

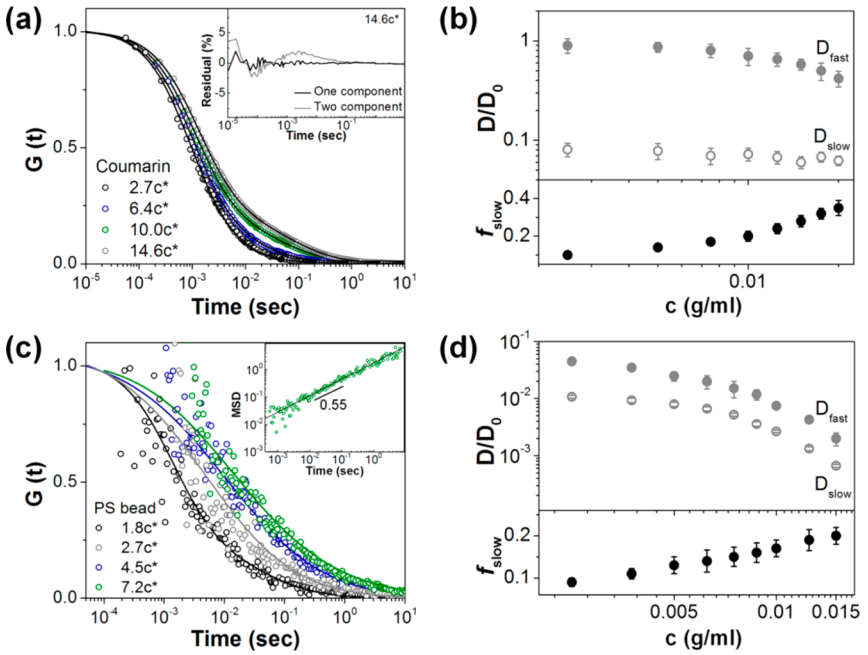

Figure 5. (a) On linear−log scales, the normalized $G(t)$ function of coumarin is plotted against time for various concentrations of gel-state methylcellulose at 70 °C as indicated in the figure. The inset shows the fit residual for one- and two-component fitting of the curve at polymer concentration 14.6c*. (b) Log−log scales. Upper panel (coumarin) shows the diffusion slowdown of two-component diffusion for the fast and slow components of D/D_0. Lower panel (coumarin) shows the amplitude of the slow component as a function of the methylcellulose concentration. (c) Log−log scales. Normalized $G(t)$ function of 20 nm PS beads corresponding at various methylcellulose concentrations in the gel state. The inset shows (log−log scales) the mean-square displacement plotted against time at methylcellulose concentration 7.2c*. (d) Log−log scales. For 20 nm carboxylated PS beads, the diffusion slowdown, D/D_0, and the amplitude of the slow component are plotted against the methylcellulose concentration.

owing to hydrophobic attraction.[28,29] This postgel structure is consistent with our observations. A slow diffusion rate can be interpreted as coumarin moving into nanovoids between the individual chains that constitute the fibrils, and a high diffusion rate can be interpreted to indicate the diffusion of coumarin into the relatively larger fibrillar meshes (Figure 6). In this scenario, our observation that D_{slow} is constant whereas the D_{fast} decreases with increasing methylcellulose concentration would imply that the size of the intrafibrillar nanovoids is unaffected by the polymer concentration and that the size of the meshes generated by the fibrils decreases with increasing concentration.

Furthermore, Figure 5c shows that the autocorrelation function of the carboxylated latex particles slows with increasing methylcellulose concentration. This presumably reflects reduced porosity of the hydrogel owing to lower gel mesh size. These data are likewise (as for coumarin) described well by a fast and slower diffusion coefficient, except that for this tracer, both D_{fast} and D_{slow} decreased with increasing methylcellulose concentration (Figure 5d). This was probably because the fibril structure offered insufficient space for the particles to diffuse within it; they could diffuse only through the larger meshes, as illustrated in Figure 6. Quantification showed that the D_{fast} and D_{slow} values differed by a factor of approximately 5—a difference much less than for coumarin. The mean-square displacement of these particles in the high-concentration regime displayed the slope of 0.55, regardless of the time. Thus, these results appear to reflect the local heterogeneity of the gel.

In conclusion, we studied tracer diffusion in methylcellulose solutions using two-photon FCS, in the case of transient mesh

dx.doi.org/10.1021/ma501331z | Macromolecules XXXX, XXX, XXX−XXX

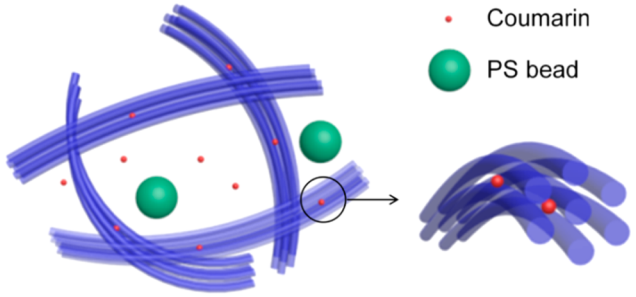

Figure 6. Schematic illustration of hypothesized methylcellulose in the gel state at 70 °C. Methylcellulose chains aggregate into fibril bundles, and these fibrils generate large meshes. The small coumarin tracers diffuse within and outside bundles but the larger 20 nm PS beads can move only within the larger meshes, as described quantitatively in this paper.

networks of the fluid state (low temperature) and with comparison to the gelled state (high temperature) in which fibrillar structures are believed to form. The observed two diffusion components in the fluid state depend simply on size of the particle relative to the polymer mesh size, which follows from standard ideas in polymer physics.[22] The more complex diffusion patterns observed in the gel state appear to reflect complexity of the gel structure. This industrially relevant polymer produces simple diffusion patterns that we find to be repeatable, obeying systematic, physically meaningful patterns described quantitatively in this paper. Developing a deeper understanding on how gel structure and additive properties relate to diffusion will aid in the development of formulations for applications such as food or pharmaceuticals where the diffusion of the ingredients can underpin performance.

AUTHOR INFORMATION

Corresponding Author

*E-mail sgranick@illinois.edu, tel (217) 333-5720; fax (217) 244-2278 (S.G.).

Notes

The authors declare no competing financial interest.

ACKNOWLEDGMENTS

We gratefully acknowledge support from the Dow Chemical University Research Program with the University of Illinois. The construction of home-built FCS instrumentation was supported by the National Science Foundation under Award DMR- 09-07018.

REFERENCES

(1) Clasen, C.; Kulicke, W. M. *Prog. Polym. Sci.* **2001**, *26*, 1839.
(2) Amiji, M.; Park, K. *Biomaterials* **1992**, *13*, 682.
(3) Li, L. *Macromolecules* **2002**, *35*, 5990.
(4) Hirrien, M.; Chevillard, C.; Desbrières, J.; Axelos, M. A. V.; Rinaudo, M. *Polymer* **1998**, *39*, 6251.
(5) Desbrières, J.; Hirrien, M.; Ross-Murphy, S. B. *Polymer* **2000**, *41*, 2451.
(6) Tong, P.; Ye, X.; Ackerson, B. J.; Fetters, L. J. *Phys. Rev. Lett.* **1997**, *79*, 2363.
(7) Won, J.; Onyenemezu, C.; Miller, W. G.; Lodge, T. P. *Macromolecules* **1994**, *27*, 7389.
(8) van der Gucht, J.; Besseling, N. A. M.; Knoben, W.; Bouteiller, L.; Cohen Stuart, M. A. *Phys. Rev. E* **2003**, *67*, 051106.
(9) Lu, Q.; Solomon, M. J. *Phys. Rev. E* **2002**, *66*, 061504.
(10) Magde, D.; Elson, E.; Webb, W. W. *Phys. Rev. Lett.* **1972**, *29*, 705.
(11) Hess, S. T.; Huang, S.; Heikal, A. A.; Webb, W. W. *Biochemistry* **2002**, *41*, 697.
(12) Saxton, M. J. *Biophys. J.* **2012**, *103*, 2411.
(13) Guo, J.; Baker, G. A.; Hillesheim, P. C.; Dai, S.; Shaw, R. W.; Mahurin, S. M. *Phys. Chem. Chem. Phys.* **2011**, *13*, 12395.
(14) Vagias, A.; Raccis, R.; Koynov, K.; Jonas, U.; Butt, H.-J.; Fytas, G.; Košovan, P.; Lenz, O.; Holm, C. *Phys. Rev. Lett.* **2013**, *111*, 088301.
(15) Alexandrakis, G.; Brown, E. B.; Tong, R. T.; McKee, T. D.; Campbell, R. B.; Boucher, Y.; Jain, R. K. *Nat. Med.* **2004**, *10*, 203.
(16) Keary, C. M. *Carbohydr. Polym.* **2001**, *45*, 293.
(17) Arvidson, S. A.; Lott, J. R.; McAllister, J. W.; Zhang, J.; Bates, F. S.; Lodge, T. P.; Sammler, R. L.; Li, Y.; Brackhagen, M. *Macromolecules* **2012**, *46*, 300.
(18) Grossman, P. D.; Soanes, D. S. *Biopolymers* **1991**, *31*, 1221.
(19) Zhao, J.; Granick, S. *Macromolecules* **2007**, *40*, 1243.
(20) Rigler, R.; Mets, Ü.; Widengren, J.; Kask, P. *Eur. J. Biophys.* **1993**, *22*, 169.
(21) Shusterman, R.; Alon, S.; Gavrinyov, T.; Krichevsky, O. *Phys. Rev. Lett.* **2004**, *92*, 048303.
(22) Cai, L.-H.; Panyukov, S.; Rubinstein, M. *Macromolecules* **2011**, *44*, 7853.
(23) Cherdhirankorn, T.; Best, A.; Koynov, K.; Peneva, K.; Muellen, K.; Fytas, G. *J. Phys. Chem. B* **2009**, *113*, 3355.
(24) Michelman-Ribeiro, A.; Horkey, F.; Nossal, R.; Boukari, H. *Biomacromolecules* **2007**, *8*, 1595.
(25) Cheng, Y.; Prud'homme, R. K.; Thomas, J. L. *Macromolecules* **2002**, *35*, 8111.
(26) Kohli, I.; Mukhopadhyay, A. *Macromolecules* **2012**, *45*, 6143.
(27) Kobayashi, K.; Huang, C.-i.; Lodge, T. P. *Macromolecules* **1999**, *32*, 7070.
(28) Lott, J. R.; McAllister, J. W.; Arvidson, S. A.; Bates, F. S.; Lodge, T. P. *Biomacromolecules* **2013**, *14*, 2484.
(29) Lott, J. R.; McAllister, J. W.; Wasbrough, M.; Sammler, R. L.; Bates, F. S.; Lodge, T. P. *Macromolecules* **2013**, *46*, 9760.